Environmental Advances 9 (2022) 100310

Contents lists available at ScienceDirect

Environmental Advances

journal homepage: www.sciencedirect.com/journal/environmental-advances

Testing specificity and sensitivity of wastewater-based epidemiology for detecting SARS-CoV-2 in four communities on Vancouver Island, Canada

Nadia Zeina Masri [a], Kiffer George Card [b], Emmanuelle A. Caws [c], Alana Babcock [a], Ryan Powell [e], Christopher J. Lowe [d], Shelley Donovan [d], Shelley Norum [e], Shirley Lyons [d], Sean De Pol [e], Lareina Kostenchuk [f], Caetano Dorea [c], Nathan J. Lachowsky [h], Stephanie M. Willerth [i,j], Thomas M. Fyles [f], Heather L. Buckley [g,*]

[a] Division of Medical Sciences, University of Victoria, Victoria, BC V8W 2Y2, Canada
[b] Faculty of Health Sciences, Simon Fraser University, Canada
[c] Department of Civil Engineering and Centre for Advanced Materials and Related Technologies (CAMTEC), University of Victoria, Canada
[d] Environmental Monitoring Program, Capital Regional District, Canada
[e] Regional District of Nanaimo, Canada
[f] Pani Energy Inc., Canada
[g] Department of Civil Engineering, Department of Chemistry, and Centre for Advanced Materials and Related Technologies (CAMTEC), University of Victoria, Canada
[h] School of Public Health and Social Policy, University of Victoria, Canada
[i] Department of Mechanical Engineering and Division of Medical Sciences, University of Victoria; Centre for Advanced Materials and Related Technologies (CAMTEC), University of Victoria, Canada
[j] School of Biomedical Engineering, University of British Columbia, Canada

ARTICLE INFO

Keywords:
qPCR
Sensitivity
Specificity
Wastewater-based epidemiology
Wastewater surveillance
SARS-CoV-2
Pepper mild mottle virus

ABSTRACT

We report wastewater surveillance of the spread of SARS-CoV-2 based upon 24-h composite influent samples taken weekly from four wastewater treatment plants (WWTP) on Vancouver Island, BC, Canada between January 3, 2021 and July 10, 2021. Samples were analyzed by reverse transcription quantitative polymerase chain reaction targeting the N1 and N2 gene fragments of SARS-CoV-2 and a region of the replication associate protein of the pepper mottle mosaic virus (PMMoV) serving as endemic control. Only a small proportion of samples had quantifiable levels of N1 or N2. Overall case rates are weakly correlated with the concentration (gene copies/L) and with the flux of viral material influent to the WWTP (gene copies/day); the latter accounts for influent flow variations. Poisson multimodal rank correlation accounts for differences between the four WWTP and shows a significant correlation with a significant positive intercept. Receiver operator characteristics (ROC) analysis confirms a cut-off of cases based on amplified/not-amplified experimental data. At the optimal cut point of 19 (N1) or 17 (N2) cases/week/100,000 the sensitivity and specificity is about 75% for N1 and 67% for N2.

Abbreviations

aRNA	Armored RNA
COVID-19	Coronavirus disease - 2019
DNQ	Detected not quantified
FC	French Creek Pollution Control Center
FN, TN	False, true negative
FP, TP	False, true positive
GN	Greater Nanaimo Pollution Control Center
LOD, LOQ	Limit of detection, quantification
MCL	McLoughlin Point WWTP
N1, N2	Sequence in the SARS-CoV-2 genome
PEG	poly-ethylene glycol precipitation method
PMMoV	Pepper mild mottle virus
ROC	Receiver operator characteristic
SARS-CoV-2	Severe Acute Respiratory Syndrome Corona virus - 2
SMF	skim milk flocculation
SP	Saanich Peninsula WWTP
WBE	Wastewater-based epidemiology
WWTP	Wastewater treatment plant

* Corresponding authors.
E-mail address: hbuckley@uvic.ca (H.L. Buckley).

https://doi.org/10.1016/j.envadv.2022.100310
Received 17 July 2022; Received in revised form 22 September 2022; Accepted 27 October 2022
Available online 28 October 2022

1. Introduction

The Coronavirus disease-2019 (COVID-19) pandemic caused by the Severe Acute Respiratory Syndrome Coronavirus 2 (SARS-CoV-2), an enveloped, positive-sense, single-stranded RNA virus has left millions of people infected and left billions of others affected. Hosts can spread SARS-CoV-2 as early as 24-h after infection during a 2-week incubation period during which symptoms may or may not present (Transmission of SARS-CoV-2: implications for infection prevention precautions 2022). The longevity and frequency of asymptomatic transmission can delay clinical testing for SARS-CoV-2 (Xagoraraki and O'Brien, 2020) and can reflect local testing resources rather than an accurate estimation of true prevalence (Majowicz et al., 2005). Accordingly, widespread community transmission can occur prior to the adoption of any appropriate precautionary action (Wu et al., 2020). These limitations have caused researchers to take alternative approaches for identifying SARS-CoV-2 in populations through active surveillance that can provide an earlier warning of an outbreak and accordingly, significantly lowering the epidemic curve (Ibrahim, 2020). Previously, wastewater testing has been central to public health responses in other infectious disease epidemics, including the near-eradication of poliovirus (Asghar et al., 2014) as well as detecting outbreaks of enteroviral and hepatitis infections (Pellegrinelli et al., 2016).

Wastewater monitoring provides an opportunity for active surveillance. Hosts infected with SARS-CoV-2 shed the virus in their fecal matter, creating the opportunity to gather data from the excreted fecal matter in wastewater for a set population (Larsen and Wigginton, 2020; Philo et al., 2022). In contrast to passive surveillance based on clinical testing, active testing of viral molecular markers in wastewater presents benefits, including (i) detecting SARS-CoV-2 from both symptomatic and asymptomatic carriers; and (ii) sampling a large portion of the population to provide better insight as to the true prevalence of SARS-CoV-2 in such populations (Mallapaty, 2020).

The most common method to detect SARS-CoV-2 is qPCR, additionally over the COVID-19 pandemic other methods have been recently used such as droplet qPCR and (PCR)-based or loop-mediated isothermal amplification (LAMP) (Ramírez-Chavarría et al., 2022; Alhama et al., 2022).

The prevalence of SARS-CoV-2 in wastewater has been correlated to clinical testing data in over 60 countries (Medema et al., 2020; Ahmed et al., 2020; Randazzo et al., 2020; COVIDPoops19 Dashboard, 2022), demonstrating the relationships between both datasets, as well as the capacity and feasibility of wastewater-based epidemiology (WBE) to provide robust data regardless of clinical testing uptake. At smaller scales, several examples exist where testing of wastewater in concrete settings has allowed proactive isolation and targeted clinical testing for impacted populations (Betancourt et al., 2021; Ahmed et al., 2021)

WBE offers potentially unbiased surveillance in areas where testing is not as readily available. Community testing applied routinely might provide a warning of virus present in the community; several authors have noted that it cannot replace standard testing (Wu et al., 2020; Michael-Kordatou et al., 2020). Many WBE studies focus on a correlation of viral concentration with case rates in the population. Such correlations are significant when relatively high case rates occur in larger population centers. A recent report of WBE in communities of different sizes across Scotland provides clear correlations of viral concentration with clinical case rates, but there was substantial variability in the significance of the correlation in smaller population centers (Fitzgerald et al., 2021).

This study explores the utility of WBE for surveillance on Vancouver Island, British Columbia, Canada between January 3, 2021, and July 10, 2021. This is a relatively low population density region that experienced a clear wave of infections in the study period. The peak infection case rate was relatively low compared with other studies (< 60 cases/week/100,000) although there were cases of the disease continually throughout the study period. Wastewater samples were collected as part of routine water quality testing from wastewater treatment plants of four municipal sewersheds. While a wealth of literature now exists regarding sample preparation and analysis strategies, surveillance methods used to inactivate, filter, concentrate and extract viral RNA and the correlating analysis by qPCR were developed based on literature and best practices available in the absence of any international consensus at the beginning of this study (O'Reilly et al., 2020). The accumulated dataset supports a variety of statistical analyses to explore correlations of case rates with viral concentrations and viral influent flux based on quantified samples. The focus is on the sensitivity and specificity of qPCR methodology for WBE as it applied in the region during the period of study.

2. Material and methods

2.1. Sampling at WWTP and Transportation

Four different sample sites were located on Vancouver Island, BC, Canada: (i) McLoughlin Point Wastewater Treatment Plant (MCL) in Esquimalt serving the core municipalities of Victoria, Esquimalt, Saanich, Oak Bay, View Royal, Langford and Colwood, and the Esquimalt and Songhees Nations; (ii) Saanich Peninsula Treatment Plant (SP) at Bazan Bay, which serves North and Central Saanich, the town of Sidney, and the Tseycum, Tsartlip, and Pauquachin First Nations; (iii) French Creek Pollution Control Centre (FC) that serves Qualicum Beach, Parksville and the service areas of French Creek, Pacific Shores, Surfside and Barclay Crescent; and (iv) Greater Nanaimo Pollution Control Centre (GN), which serves the City of Nanaimo, Snuneymuxw First Nation, and the District of Lantzville. Influent composite samples (500 mL) were collected in sterile Nalgene bottles using ISCO 5800 automated samplers (Teledyne ISCO, Lincoln, NE, USA) at GN, FC, and SP. Time-based composite samples were collected over 24 h (every 15 min at GN and FC, every 30 min at SP). At MCL, 24-h flow-proportional composite influent samples (500 mL) were collected in sterile Nalgene bottles using an Endress+Hauser CSF48 (Endress+Hauser AG, Switzerland) automated sampler. Sampling occurred once per week between January 2021 and July 2021 at all four sites. Once the samples were collected, they were transported on ice and stored at 4 °C and processed within 48 h of receipt.

2.2. Virus concentration and RNA extraction

The samples were inactivated by a 30-min cycle under two 15W germicidal UV-C fluorescent light bulbs followed by 90 min in a bead bath using Lab Armor™ Beads (Cat. No. A1254301, Thermo Fisher, Waltham, MA, USA) at 60 °C. The virus was concentrated using two different methods: poly-ethylene glycol precipitation (PEG) (Developing a Wastewater Surveillance Sampling Strategy, 2022) and skim milk flocculation (SMF) (Philo et al., 2022).

Method 1- PEG Precipitation: 40 mL of inactivated sample was decanted once solids were settled and added to a 50 mL centrifuge tube containing 4 g of polyethylene glycol 8000 (PEG 8000) (Cat. No. P2139, EMD Millipore, Burlington, MA, USA) and 0.9 g of Sodium Chloride (NaCl). This process was repeated twice per sample site to a total of 80 mL. The samples were vigorously shaken by hand then placed on ice and shaken at 100 rpm for 1 h. The samples were left at 4 °C overnight, followed by two hours of centrifugation at 12,000 x g at 4 °C. The supernatant other than approximately 1 mL was poured out and the pellets were resuspended in the remaining liquid using a pipette, vortexed then transferred to a 1.5 mL microfuge tube. The samples were then centrifuged for 5 min at 12,000 x g. The supernatant was completely removed. The pellets were flash frozen in liquid nitrogen and stored at −80 °C until ready to be further processed. The extra wastewater samples that were not concentrated were decanted into 50 mL centrifuged tubes, flash frozen and placed at −80 °C.

Method 2- Skim Milk Flocculation: 40 mL of 5% skim milk (w/v) solution was made using Skim Milk Powder (Cat. No. OXLP0031B,

Thermo Fisher, Waltham, MA, USA) and dissolved completely in distilled water. Once dissolved, the milk solution was autoclaved for 15 min. 2.5 mL of autoclaved skim milk solution was added to 250 mL wastewater sample (10% of the skim milk solution to sample volume).

The pH of the samples was adjusted with 1 M hydrochloric acid (HCl) to a pH of 3-4. The samples were shaken for 2 h at 200 rpm at room temperature, then poured into 50 mL centrifuge tubes and centrifuged for 30 min at 4 °C at 3000 x g. The supernatant was discarded from all samples and the pellets from the tubes were pooled and resuspended in 3 mL PBS and transferred to a 15 mL conical tube and vortexed and stored at −80 °C until needed.

The All Prep PowerViral DNA/RNA Kit (Cat. No. 28000-50, Qiagen, Germantown, MD, USA) was used for the RNA extractions. For method 1, the pellets were suspended in 300 μL of PM1/2-Mercaptoethanol solution. Two pellets from each site were then combined. For method 2, a 200 μL sample was mixed with 600 μL PM1/2-Mercaptoethanol solution. Instructions were followed per the manufacturer's instructions with some minor modifications with the addition of 600 μL of anhydrous ethanol to help precipitate the RNA out of the solution. The final pellet was eluted in 30 μL RNAse/DNAse-free water and incubated for 10 min at room temperature before the final centrifugation step at 13,000 x g for 1 min. The RNA pellet was placed at −80 °C until ready for further processing.

2.3. qPCR

One-step RT-qPCR was performed using Luna® Probe One-Step RT-qPCR 4X Mix with UDG (Cat. No. M3019E, New England Biolabs, Ipswich, MA, USA) to analyse N1 and N2 gene fragments of SARS-CoV-2 (2019-nCoV RUO Kit) (Cat. No. 10006713, IDT, Coralville, IA, USA) and PMMoV (IDT, Coralville, IA, USA). All RT-qPCR amplifications were performed in 10 μL reactions. All RT-qPCR amplifications were performed in 10 μL reactions. The following mastermixes were made: (i) N1, containing forward and reverse primers concentrations of 400 nM each and the probe at a concentration of 125 nM; (ii) N2, containing forward and reverse primers at concentrations of 400 nM each and the probe at a concentration of 125 nM; and (iii) PMMoV, containing forward and reverse primers at concentrations of 500 nM each and the probe containing affinity plus beads at a concentration of 125 nM. 1 μL of RNA sample was added per reaction. Sequences of the primers and probes are shown in Table S1. For method two (skim milk), the samples were run both undiluted and with a 1:4 dilution, diluted in RNAse/DNAse free water. For quantification, a relative standard curve was made on each plate using SARS-CoV-2 Standard (Cat. No. COV019, Exact Diagnostics, Fort Worth, TX, USA) or Armored RNA (aRNA) Quant SARS-CoV-2 (Cat. No. 52030, Cedarlane, Burlington, ON, Canada) with a 5 series dilution ranging from 6.25 copies/μL to 100 copies/mL for N1 and N2 and 5 series dilution of a DNA gBlock Gene Fragment (IDT, Coralville, IA, USA) for the PMMoV standard starting at 1.524×10E6 copies/μL to 152.4 copies/μL. Each standard curve included a no template control using RNAse/DNAse free water. All samples and standards were run in triplicate. The RNA was released from the aRNA before adding the sample to the plate by heat lysis at 75 °C for 5 min. Using the Applied biosystems StepOnePlus qPCR machine (Thermo Fisher, Waltham, MA, USA), the cycling conditions were 25 °C for 30 s to prevent carryover, 55 °C for 10 min to initiate reverse transcription, 95 °C for 1 min for initial denaturation, and 45 cycles at 95 °C for 10 s and 55 °C for 1 min for the denaturation and extension steps, respectively. Only samples that had no detection for the NTC and were positive for the PMMoV were accepted.

2.4. qPCR data handling

The instrument datafile for export consisted of header information and 96 data rows that included a sample identifier and its measured C_T value, mean and standard deviation of identified triplicate wells, and flags reporting checks done on the baseline, the amplification, and the threshold; any failed flags set the measured C_T value for the well as "undetermined". No calibration data or statistical information was available for export. The export file was processed using python scripting to isolate the calibration information for each target, identify and remove any "undetermined" wells, generate a calibration curve by linear regression of C_T as f(log (copies/well)), and determine regression statistics. The results matched the limited calibration information for the datafile viewed by the instrument internal software; the reported mean and standard deviation were correctly calculated within the instrument. The instrument datafile was processed to isolate the sample data rows (identifier, measured C_T including any "undetermined" values of C_T, C_T mean and standard deviation, flags indicating experiment failure).

The calibration limit of detection (LOD) in qPCR has been extensively discussed and statistically robust methods have been recommended (Ellison et al., 2006; Forootan et al., 2017). Unfortunately, our survey is based on triplicate wells from a single sample which do not support in-depth statistical methods. We follow earlier suggestions of (Burns and Valdivia (2007) and Ellison et al. (2006) that tie to a conventional chemical analysis (Shrivastava and Gupta, 2011) and are related to logistic models as recommended in Forootan et al. (2017). The LOD is determined from the ratio of the standard error (SE) and the absolute value of the slope (m) of the regression (calibration LOD = 3 SE/|m|). Following convention, the calibration limit of quantification (LOQ) = 10 SE/|m|. The semi-log calibration values are converted to copies/well via the antilog.

The associated calibration slope and intercept, regression information (r-squared, standard error), calibration limit of detection and limit of quantification (LOD, LOQ) was appended to each row. Additional flags were appended to identify sample non-detects (ND) and detected-not-quantified (DNQ) based on the calibration LOD/LOQ. Processed sample rows were appended to a primary datafile containing all qPCR results.

The sample identifier allowed additional fields to be appended to each row to separately identify the sample location, sample date, and the method used for RNA isolation. The method further identified the sample dilution factor and its uncertainty which were appended to each sample row. This in turn allowed the calculation of the measured copies/well and the associated uncertainty, the measured copies/L of influent and its uncertainty, and the method LOD/LOQ as it applied to the sample.

Retrospectively the calibration statistical information was examined using a control-chart approach to identify periods where the analytical process was under effective control for each of the three targets (N1, N2, PMMoV). After an initial period of method refinement, most analyses appeared acceptable with few outliers. The quality of the calibration as reflected in the qPCR efficiency ($10^{-1/m}$ -1), the r-squared value, or the standard error all indicated the same subset of suspect calibrations. We chose a standard error of 0.8 (log copies/well) as an upper limit of acceptance of the analytical data corresponding to LOD < 8 copies/well. The datafile was filtered to remove samples associated with unacceptable calibrations based on the standard error. In most cases, an unacceptable calibration with one target also had unacceptable calibrations with other targets. Additional filtering removed replicate rows to give unique rows for station, date, and target. Most samples produced values for all three targets.

2.5. Sewershed and epidemiological data handling

The sewersheds are located in the Capital Regional District (CRD) and Regional District of Nanaimo (RDN). Maps of the sewersheds and populations served at each WWTP were produced by CRD and RDN. The Vancouver Island Health Authority (VIHA) is subdivided into Local Health Authorities (LHA) and further subdivided into Community Health Service Areas (CHSA). VIHA provided case data by CHSA based on episode reporting (reported date of first symptoms or date of first

positive test result) within a defined epiweek (Sunday – Saturday). Historically, the sewersheds and the CHSAs are associated with municipal and other local boundaries so there is an overlap of CHSA boundaries with sewershed boundaries. However, rural properties within a CHSA may not be served by the associated sewersheds. The rural proportion in the CHSAs that comprise the Greater Victoria and Greater Nanaimo sewersheds is less than 2%. The Saanich Peninsula WWTP serves three CHSA. One of these (Town of Sidney) is fully served by the SP sewershed. A second (North Saanich) is 45–55% served by the sewershed with the balance on rural septic systems; the case counts from the North Saanich CHSA were scaled by 50%. The third CHSA (Central Saanich, population 19,330) is 80–85% served by WWTPs with the balance on rural septic systems. No scaling of the case counts was done to correct for the rural population. The Tsawout First Nation, whose population of 1,600 lies within this CHSA, operates an independent WWTP. In the absence of finer grained case data, cases that may have occurred within this subpopulation are included in the case total for this CHSA even though they would not contribute to the viral loading at the SP WWTP. The French Creek WWTP serves two municipalities - Parksville and Qualicum - that are almost entirely on the sewershed. The WWTP is in an unincorporated area of French Creek between the two urban centers and serves an additional population of approximately 1000 not associated with either municipality. The case counts for this subpopulation are included in the Oceanside Rural CHSA (population 24,930). The Oceanside Rural case counts were not included so any cases in the French Creek subpopulation are not included in the total for the WWTP.

The total cases by epiweek were determined for each of the WWTPs and were converted to cases per week per 100,000 population based on the populations served by the sewershed. Most samples were collected from Sunday to Monday, so the sample dates were assigned to the preceding week.

4. Results and discussion

4.1. Characteristics of the dataset

The available data has several internal characteristics:

1) Influent samples (24-h composites) were obtained as subsamples of regulatory monitoring from four WWTP. While we used 24-h composite influent wastewater samples, recent research suggests that sampling sludge contains a majority of the enveloped virus (Balboa et al., 2021) especially if clinical case counts are low (Balboa et al., 2021; Developing a Wastewater Surveillance Sampling Strategy, 2022). Collecting solids requires specialized equipment that was not uniformly available at the four sampling locations (Fitzgerald et al., 2021; D'Aoust et al., 2021). Our sampling was aligned with pre-existing regulatory and operational sampling methods used for monitoring by the WWTP operators. Although these four sources represent roughly half the population of Vancouver Island, they differ in numbers of clients served by a factor of ten (Mcloughlin Point Greater Victoria. 300,000, MCL; Greater Nanaimo, 100,000, GN; Saanich Peninsula, 33,000, SP; French Creek, 28,000, FC). The case rates for each sewershed are derived from Community Health Service Area (CHSA) data that generally overlap sewershed areas but include significant rural populations not served by the SP and FC WWTPs.

2) The samples were fractionated by two different methods based on either skim milk fractionation (SMF; 34% of samples) (Philo et al., 2022) or PEG precipitation (PEG, 66%) (Wu et al., 2021). Within each type there were differences in initial, reconstitution, and final elution volumes as methods were refined. Roughly 90% of the samples in the final dataset were processed with one of two closely related PEG methods or one of three closely related SMF methods. Since the volumes and volumetric precision within each method varies, the propagated dilution factors varied; the propagated volumetric uncertainties were relatively constant (8.0 – 8.2% RSD).

3) Three targets were analyzed. N1 and N2 primer sequences for SARS-CoV-2 (Real-time RT-PCR Primers and Probes for COVID-19; CDC 2022) targeting the nucleocapsid gene and the primer sequence targeting the replication associated protein for PMMoV. A calibration curve was made for each individual qPCR plate: each qPCR analysis contained one calibration dilution sequences for all three targets, and each set of samples was determined relative to the calibration from the same qPCR analysis. Day-to-day variations in the slope, intercept, and regression statistics of the linear C_T as f(log copies/well) calibration were monitored and provided the limit of detection (LOD) and limit of quantification (LOQ) for each sample. Samples that failed to amplify or were amplified to a level below the LOD were flagged as not detected (ND); samples amplified to a level between the LOD and LOQ were flagged as detected not quantified (DNQ). Retrospectively, calibrations were examined to reject those that lay outside a control chart band based on 90% probability of the mean of the standard errors in y of the regression. Within the accepted dataset the uncertainty in the qPCR replicates on a single plate is 16% RSD.

We had anticipated using PMMoV normalized values of N1 and N2 concentrations as others have employed (Feng et al., 2021; D'Aoust et al., 2021). PMMoV is a non-enveloped, positive-sense, single stranded RNA virus that is known for its extraneous stability and for being the most abundant human virus shed through stool resulting in its prevalence in sewer systems globally (Symonds et al., 2018; Kitajima et al., 2018). Using a gene sequence from the replication-associated protein for amplification, PMMoV concentrations show little seasonality making it a useful fecal indicator (Symonds et al., 2018). In the event, the dataset contains a large proportion of ND and DNQ samples for SARS-CoV-2 targets N1 and N2. Table 2 gives an overview of the dataset from the perspective of the numbers of samples available, detected, and quantified. The PMMoV target was quantified in all samples done in parallel with the N1/N2 targets. Fig. 1 panel A includes PMMoV values from 125 independent samples and replicates for the four sewersheds. There are a few outliers, but the values are generally clustered with only a small trend to higher values during the period (dashed line). The histogram distribution of values (Fig. 1 panel B) is log-normal (r-sq = 0.978) with a mean of log (PMMoV gc/L) = 7.48 ± 0.34.

At the time of the study design – during summer and fall of 2020 - we did not have access to a reference virus, such as 299E, OC43 bovine coronavirus (BCoV) to assess recovery efficiency of the methods. However, using aRNA added to samples that were otherwise ND for both N1 and N2 suggest a recovery of 7.0 ± 2.4% (RSD 34%). These spiked samples have a mean PMMoV concentration of log(copies PMMoV) = 7.47 indicating that the spiked experiments were consistent with the larger population of samples. A current challenge with WBE for COVID-19 remains the lack of standard protocols for each step in the methods (Ibrahim, 2020; Pulicharla et al., 2021; Shah et al., 2022) but interlab studies show that different methods can be used to give comparable outcomes (Developing a Wastewater Surveillance Sampling Strategy, 2022; Phase 1 Inter-Laboratory Study – Canadian Water Network, 2022). Here, the PMMoV replicates show no significant differences between the two fractionation methods (SMF or PEG). Replicate samples analysed on the same plate have a relative uncertainty of ± 24% in the mean, consistent with the propagated uncertainty in the individual

Table 1
Population size of each WWTPs and their flow data.

WWTP	FC	GN	MCL	SP
Sewershed Population estimated	28,200	100,781	297,935	32,611
Census Population (2021)	31,054	103,680	322,245	41,938
Assumed population	28,000	100,000	300,000	33,000
Mean influent flow m^3 /day	9992	29,228	90,256	8721
Maximum flow in period m^3/day	12,838	53,503	149,429	11,989
Minimum flow in period m^3/day	9041	21,925	45,829	7802

Table 2
Numbers of samples from four WWTPs and the counts of quantified, detected not quantified (DNQ) and not detected (ND) samples for N1 and N2 SARS-CoV-2 primer sequences for the period January 3 to July 3, 2021 (epiweeks 1–26).

station	N1 samples	N1 quantified	N1 DNQ	N1 ND	N2 samples	N2 quantified	N2 DNQ	N2 ND
FC	37	4	1	32	36	2	0	34
GN	37	3	10	24	41	6	5	30
MCL	34	5	3	26	32	1	5	26
SP	35	4	1	30	35	2	2	31
total	143	16	15	112	144	11	12	121

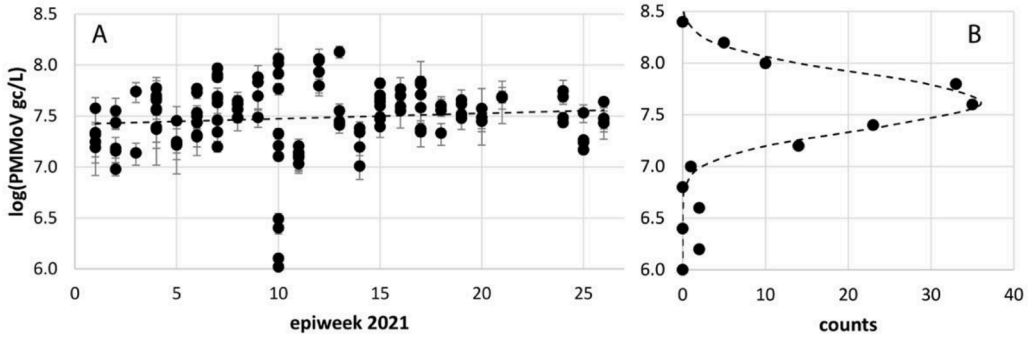

Fig. 1. A (left) PMMoV genome copies/L (logarithmic scale) as a function of epiweek 2021. Errors bars give sample uncertainty. Dashed line is a linear least-squares fit to the dataset. B (right) Histogram of counts on an interval of 0.15 log(PMMoV gc/L). Dashed line is the least-squares fit to a Gaussian, $R^2 = 0.51$.

analyses (16%) and the volumetric precision of the extraction (8%). Replicate samples from independent methods and/or independent extractions of a common field sample have an uncertainty of ± 34% RSD. This value aligns with the spiked sample uncertainty. We conclude that the internal consistency of the PMMoV portion of the dataset mirrors the internal consistency of the N1 and N2 values quantified.

Fig. 2 shows the time distribution of quantified and detected samples together with an indication of the LOD for the ND samples; an equivalent figure for N2 is given as supporting information. The quantified samples comprise only 10% (N1) or 7.6% (N2) of the total samples analyzed. With the DNQ samples included, the detected samples comprise 22% (N1) or 16% (N2) samples.

4.2. Correlation of SARS-CoV-2 markers and case rates

Fig. 2B shows the overall case rate (cases per week per 100,000 population) as it applies to the 461,000 clients served by the four sewersheds. During the period of the "Delta wave" overall case rates did not exceed 60 per 100,000 and fell to less than 2 per week at the end of the period (6–7 cases/day/100,000) on Vancouver Island as a whole. While health data show the presence of cases, this is not always observed in our data. Some of the cases on Vancouver Island occurred in places where a proportion of the population live outside sewershed service areas within a CHSA. This discrepancy will not allow the sampling at the WWTP to have a clear overlap with the population case rate in that specific area. Focusing only on the timing of quantified samples in the whole dataset, there may be a correlation between overall case rates and the concentration of the target quantified.

Fig. 3 panels A and B show a correlation of the observed concentrations as a function of the overall case rate of the region (filled circles with error bars). The slope of the correlation is relatively flat and the extrapolated intercept implies a viral concentration in the absence of cases. This type of behavior was noted by Fitzgerald et al. (2021) for similar sized WWTPs in Scotland. Fitzgerald et al noted that the concentration observed was in part dependent upon the influent flow at the various sampling locations and times and recommended the use of influent flux to correct for this variation (flux = influent flow during the sampling period x measured concentration). Testing flux is beneficial as it accounts for weather (the abundant amount of rainfall the Vancouver Island gets) and the flow of larger WWTPs thus, better representing each station.

Fig. 3 panels C and D give the correlation of influent flux as a function of total cases. These latter correlations are more acceptable in the sense that the intercept in the case of N1 is close to zero, but there is considerable scatter. The number of quantified samples is simply too low to support this type of direct correlation of our data.

Fig. 3 also includes samples that were detected but not quantified as they fell between the method LOD and LOQ. These values appear to lie mostly within the confidence interval of the weak correlation with quantified samples. We cannot include the values as part of a direct correlation but could explore the data using rank correlations based upon the relative ranking of the values, rather than their magnitude. Spearman rank correlation gave rho = 0.3142 ($p = 0.0852$) for N1 and rho = 0.5205 (p=0.1089) for N2. These values indicate a weak correlation.

The overall dataset includes data from four independent WWTPs and, as shown in Fig. 2, the progress of the "wave" of cases differed between the four locations in the period. The effect of this additional source of variance was examined using a Poisson generalized linear mixed model fit by maximum likelihood (Laplace Approximation; glmerMod() function in R) to account for clustering across the sewersheds. The flux data were scaled by a factor of 10^8 to reduce their magnitude for modelling while preserving the rank order. Table 3 gives the model outputs. Two features are significant: (i) the slope (flux correlated by cases) is significant (N1) or highly significant (N2); and (ii) the intercepts (cases in the absence of a viral flux) are positive and highly significant for both markers. These both agree with the visual summary of Fig. 3C and D.

The very high proportion of samples not detected includes two types of samples. The first are those samples which were not amplified in the PCR. Whether these samples are not amplified due to some experimental mishap, or due to the true absence of viral target in the sample, is immaterial; these are truly not detected. A second smaller group of samples are those where there is some amplification of the viral target from the sample, but the extent of amplification is insufficient to meet the analytical acceptance criteria applied. These samples are screened out at the instrument level when the amount of amplification fails to reach a set C_T limit, or the number of amplified wells in the replicates is

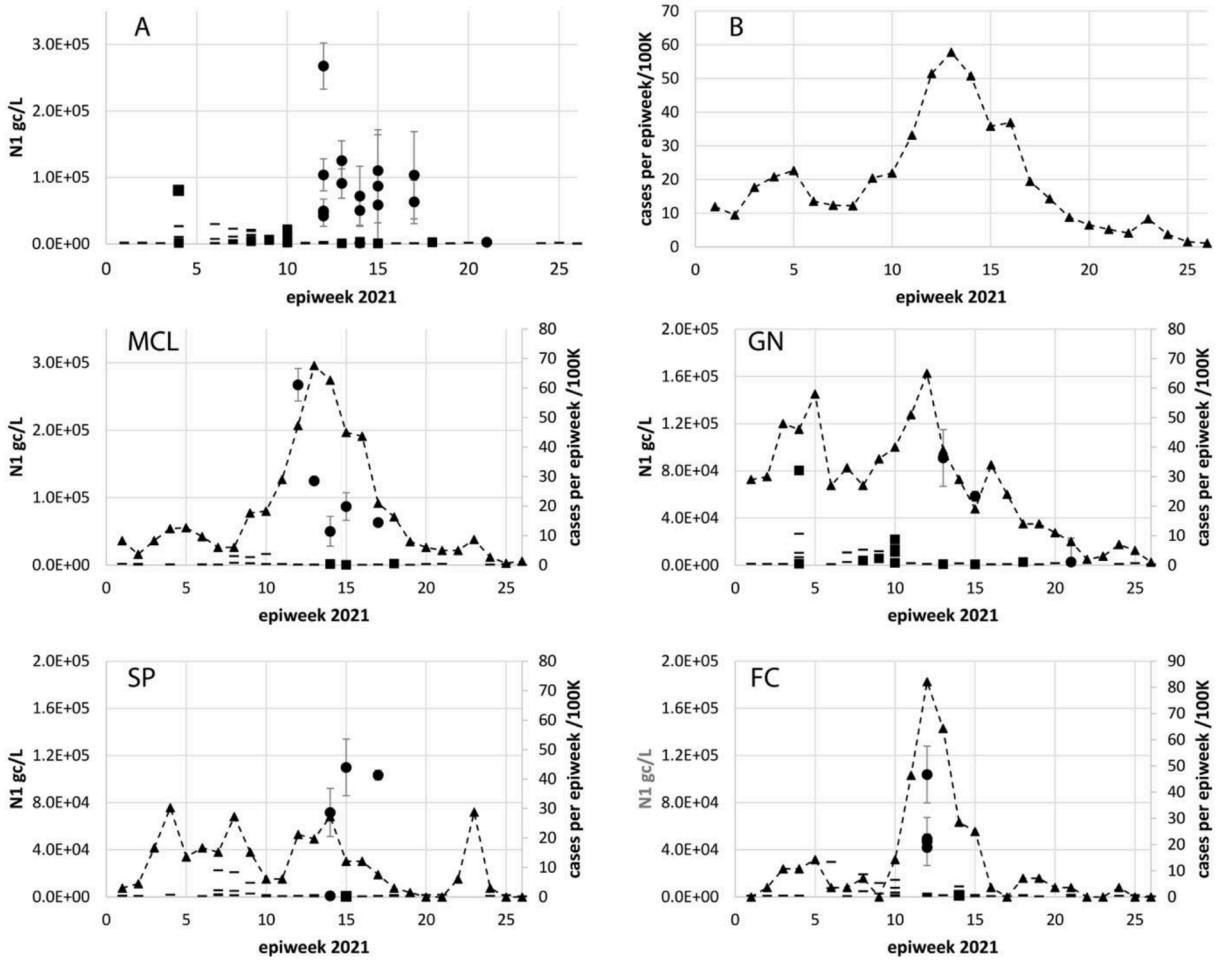

Fig. 2. Measured concentration of N1 and of COVID-19 case rates as functions of time. Quantified samples are given as circles with error bars; detected not quantified samples are given as squares at the measured value; method detection limits for not detected samples are given as horizontal bar symbols. Case data (cases per epiweek per 100,000 population) are given as triangle symbols with dashed lines to visually indicate the profiles. Panel A – all concentration data for N1 from the 4 WWTPs; panel B – combined case rates for the full population of sewershed clients; MCL – McLoughlin Point (Greater Victoria) samples and cases; GN – Greater Nanaimo samples and cases; SP – Saanich Peninsula samples and cases; FC – French Creek (Parksville-Qualicum Beach) samples and cases.

fewer than three. These are further screened by the analytical detection limit; a sample may have been amplified in three replicates, but the value is lower than the limit of detection. These samples are amplified but were counted the same as the not detected samples in Table 2. Table 4 gives the counts of samples simply in terms of amplified or not amplified by PCR based all three triplicate samples giving an accepted C_T value at the instrument. The overall proportion of amplified samples is 32% for N1 and 28% for N2, a significant increase from the more stringent analytical focus on quantified samples (11% and 8% for N1 and N2 respectively).

A focus on amplified/not amplified requires a shift in perspective to binary statistics to explore the utility of the dataset. This is akin to binary diagnostic testing where a test result (positive/negative) is used to infer the level of a continuum parameter (cases) with respect to a cut-off value. In this context, we know that there was some level of COVID-19 infection throughout the period at all sample locations. A perfect diagnostic would return the result “amplified” for most of the samples. In our real case the question is – what level of cases is required to ensure viral material is amplified in PCR? The optimum cut-point in case rate was determined by optimization of the area under the Receiver Operating Characteristic (ROC) curve. The cupointr() function in R was used for the ROC analysis and to calculate the Youden statistic to identify the optimal cut point for the number of cases needed from the case rate data to detect a positive result in the sample. The ROC curve plots the sensitivity as a function of (1- specificity) (Fig. 4). A highly specific and sensitive diagnostic ROC curve will approach the (1,0) corner of the plot; a non-specific and insensitive diagnostic will produce a curve on the diagonal.

The analysis computes true and false positives and negatives at the optimal cut-point (N1 19, N2 16.3 cases/week/100K). True positives (TP; N1 36, N2 31) are observations where the sample is amplified, and is correctly identified above the cut-point. False negatives (FN; N1 10, N2 10) are samples which are amplified but incorrectly classified above the cut-point. True negatives (TN; N1 72, N2 65) are observations of non-detects correctly identified as less than the cut-point. False positives (FP; N1 25, N2 38) occur as non-detects incorrectly classified less than the cut-point. Sensitivity (TP/(TP+FN) at the cut-point is 0.783 or 0.756 for N1 or N2 respectively. Specificity (TN/(TN+FP) at the cut-point is 0.742 or 0.631 for N1 or N2 respectively. The Youden J (Sensitivity + Specificity -1) reaches a maximum at the optimal cut-point (N1 0.525, N2 0.387). The overall accuracy ((TP+TN)/total observations) is 0.755 for N1 and 0.667 for N2.

The ROC analysis is consistent with the analysis of the quantitative data given above. The non-zero intercept of the Poisson analysis strongly indicates that our method cannot detect cases below some threshold. Above that threshold, cases are correlated with detected samples based on the observed influent flux. The binary ROC analysis indicates that there is an optimal cut-point of cases per 100,000 per week based on the binary sorting of the dataset into amplified and non-amplified samples.

At the optimum, this binary decision provides an accuracy of 75% for

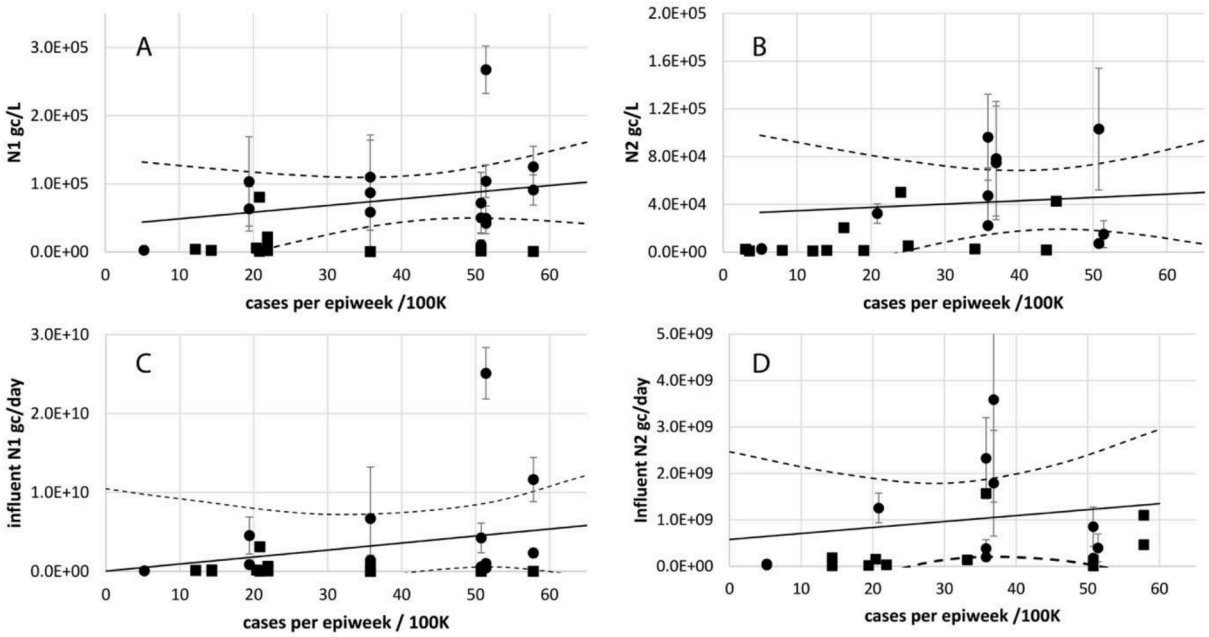

Fig. 3. Measured concentrations and influent flux of N1 and N2 as function of overall case rates for the full dataset. Quantified samples are given as circles with error bars; detected not quantified samples are given as squares at the measured value; solid line is a linear regression fit with the dashed lines showing the confidence interval ($p = 0.05$). Panels A and B give measured concentrations of N1 or N2 respectively. Panels C and D give influent flux of N1 or N2 respectively.

Table 3
Poisson generalized linear model of detected N1 and N2 samples for four sewersheds. Significance indicated by *** for highly significant or * for significant at 0.05.

	N1	N2
Intercept ± se	3.57 ± 0.501	3.11 ± 0.504
	p = 1E−12 ***	p = 6E−10 ***
Slope ± se	0.00121 ± 0.00061	0.0108 ± 0.00291
	p = 0.0477 *	p = 2E−4 ***
Observations	31	23

N1 or 67% for N2. That difference is probably significant based on the lower specificity of N2 relative to N1. The observed difference in cut-points (19 and 16.3 for N1 and N2 respectively) is probably not significant as the Youden J passes through a broad maximum between 16 and 20 cases per week/100,000 for both targets. The ROC analysis is limited by the number of unique values of case counts. Although the dataset includes over 140 samples each for N1 and N2 (Table 2), between the four stations there are only 58 unique values of cases per week/100,000. This is adequate for Fig. 4 but limits analysis of individual WWTP results where as few as 10 unique values of cases are available at some stations.

Robust exploration of the cut-off value to apply to individual WWTPs would require significantly more cases than were experienced on Vancouver Island, a longer duration study and increased samples per week. Feng et al suggest that a minimum of two samples a week are needed to maintain a reliable trend analysis (Feng et al., 2021). Additional work will be required to establish if a site-specific ROC curve for each WWTP is required. It is clear that a richer dataset will be required to explore beyond the weekly survey results we report.

5. Conclusion

We can draw two types of general conclusions from the data presented. The first is the value of influent viral marker flux (copies/day) in place of the more usually reported use of viral marker concentrations (copies/volume). Our results strongly support the suggestion of Fitzgerald et al. (2021) that flux provides a direct normalization across multiple locations. In our case, the seasonal variation of influent flow is correctly removed from the variance in the concentration data as seen in the near-zero intercept in the correlation of case rates and viral flux. Normalization with measured PMMoV is an indirect method to make this type of correction; direct use of WWTP data appears more effective.

The second conclusion is the identification of a cut-point in cases below which both the sensitivity and the specificity of the method decline to make the positive identification of cases from measured marker amplification unreliable. The actual values we determine are of lesser value than the clear indication that there is a lower limit of cases that can be identified from WBE data. Analytical limits of detection and quantification apply to WBE above some threshold; the ROC analysis, based solely on amplified/not amplified within defined instrument criteria, points to an effective lower limit of identification of cases by WBE methods. In regions with high population density, large volume WWTPs, and high case rates, quantitative correlations are possible. In regions like ours – lower population density, smaller volume WWTP - and periods of low disease incidence, identification of cases from WBE

Table 4
Numbers of samples from four WWTPs and the counts of amplified and not amplified samples for N1 and N2 SARS-CoV-2 primer sequences for the period January 3 to July 3, 2021 (epiweeks 1–26).

	N1 amplified	N1 not amplified	N1 proportion amplified	N2 amplified	N2 not amplified	N2 proportion amplified
FC	7	30	19%	4	32	11%
GN	18	19	49%	18	23	44%
MCL	12	22	35%	11	21	34%
SP	9	26	26%	8	27	23%
all	46	97	32%	41	103	28%

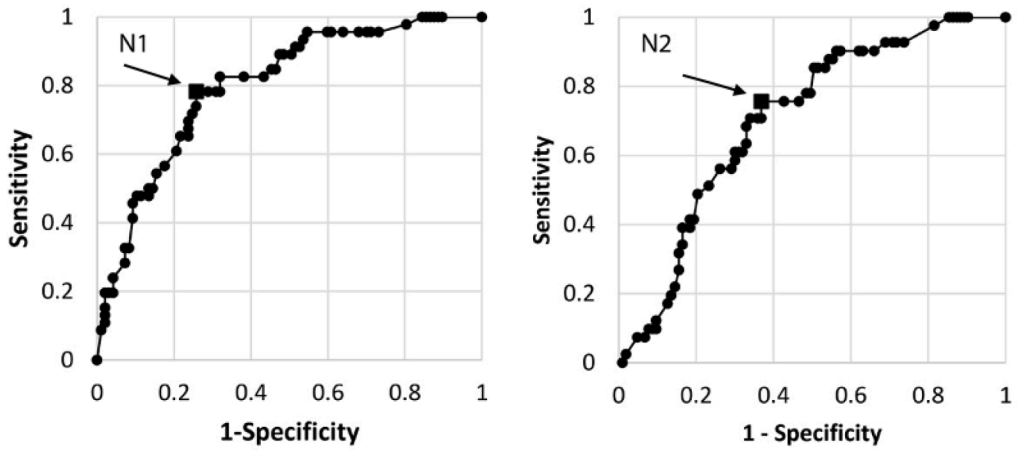

Fig. 4. Receiver Operating Characteristic (ROC) curves for PCR-amplified samples for N1 and N2 SARS-CoV-2 primer sequences for the period January 3 to July 3, 2021 (epiweeks 1–26). The arrow points to the Youden J value at the optimum cut-point which is given as the filled square. The cut point is 19 and 16.3 for N1 and N2 respectively.

will be reliable only above a cut-point above which we expect quantitative correlations to apply (Table 1).

CRediT authorship contribution statement

Nadia Zeina Masri: Data curation, formal analysis, funding acquisition, investigation, methodology, project administration, validation, visualization, writing – original draft, writing – review and editing. **Kiffer George Card:** Data curation, formal analysis, methodology, software, validation, visualization, writing – original draft, writing – review and editing. **Emmanuelle A. Caws:** Data curation, formal analysis, investigation, methodology, project administration, validation. **Alana Babcock:** investigation, methodology, validation. **Ryan Powell:** Data curation, investigation, methodology. **Christopher J. Lowe:** funding acquisition, project administration, resources. **Shelley Donovan:** investigation, project administration. **Shelley Norum:** investigation, project administration. **Shirley Lyons:** investigation, methodology, project administration. **Sean De Pol:** funding acquisition, project administration. **Lareina Kostenchuk:** funding acquisition, project administration. **Caetano Dorea:** funding acquisition. **Nathan Lachowsky:** formal analysis, funding acquisition, methodology. **Stephanie M. Willerth:** Conceptualization, funding acquisition, methodology, project administration, resources, writing – review and editing. **Thomas M. Fyles:** Conceptualization, data curation, formal analysis, funding acquisition, methodology, project administration, resources, software, validation, visualization, writing – original draft, writing – review and editing. **Heather L. Buckley:** Conceptualization, funding acquisition, methodology, project administration, resources, writing – review and editing

Declaration of Competing Interest

The authors declare that they have no known competing financial interests or personal relationships that could have appeared to influence the work reported in this paper.

Acknowledgments

The authors gratefully acknowledge the active sampling and logistical support of the Capital Regional District (Crystal Fudge & McLoughlin Point/Saanich Peninsula WWTP operations staff) and the Regional District of Nanaimo, and the Vancouver Island Health Authority for providing epidemiological data. Scott Meschke (UWash), Ryan Ziels (UBC), Natalie Prystajecky (BCCDC), Melissa Glier (BCCDC), Kara Nelson (UC Berkeley) and their teams provided critical feedback in the early stages of methods development. Funding support from the COVID 19 research program of NSERC Alliance, and personnel support funding from Technation and Biotalent funding programs is also acknowledged. SMW acknowledges the support of the CRC program. KGC was supported by a Michael Smith Health Research BC Scholar Award [#SCH-2021-1547]. Equipment was purchased with a Canadian Foundation for Innovation John Evans Leaders Foundation Grant (HLB). The Centre for Advanced Materials and Related Technologies provided facilities for the project.

Alana Babcock, Josie Chrenek, Rebecca Kircsh, Jacob Morris and Daniel Wallis provided essential technical support in sample processing. Benjamin McClennon and Gordon Wong assisted with scripting to semi-automate the retrieval of information from instrument results files.

Supplementary materials

Supplementary material associated with this article can be found, in the online version, at doi:10.1016/j.envadv.2022.100310.

References

Ahmed, W., et al., 2020. First confirmed detection of SARS-CoV-2 in untreated wastewater in Australia a proof of concept for the wastewater surveillance of COVID-19 in the community. Sci. Total Environ. 728 https://doi.org/10.1016/J.SCITOTENV.2020.138764. Aug.

Ahmed, F., et al., 2021. First detection of SARS-CoV-2 genetic material in the vicinity of COVID-19 isolation Centre in Bangladesh variation along the sewer network. Sci. Total Environ. 776 https://doi.org/10.1016/J.SCITOTENV.2021.145724. Jul.

Alhama, J., Maestre, J.P., Martín, M.Á., Michán, C., 2022. Monitoring COVID-19 through SARS-CoV-2 quantification in wastewater progress, challenges and prospects. Microb. Biotechnol. 15 (6), 1719–1728. https://doi.org/10.1111/1751-7915.13989. Jun.

Asghar, H., et al., 2014. Environmental surveillance for polioviruses in the Global Polio Eradication Initiative. J. Infect Dis. 210, S294–S303. https://doi.org/10.1093/INFDIS/JIU384. Suppl 1Nov.

Balboa, S., et al., 2021. The fate of SARS-COV-2 in WWTPS points out the sludge line as a suitable spot for detection of COVID-19. Sci. Total Environ. 772, 145268 https://doi.org/10.1016/J.SCITOTENV.2021.145268. Jun.

Betancourt, W.Q., et al., 2021. COVID-19 containment on a college campus via wastewater-based epidemiology, targeted clinical testing and an intervention. Sci. Total Environ. 779, 146408 https://doi.org/10.1016/J.SCITOTENV.2021.146408. Jul.

Burns, M., Valdivia, H., 2007. Modelling the limit of detection in real-time quantitative PCR. Eur. Food Res. Techno. 226 (6), 1513–1524. https://doi.org/10.1007/S00217-007-0683-Z. Jul. 2007.

"COVIDPoops19 Dashboard | covid19wbec.org." https://www.covid19wbec.org/covidpoops19 (Accessed 28 March 2022).

D\'Aoust, P.M., et al., 2021. Quantitative analysis of SARS-CoV-2 RNA from wastewater solids in communities with low COVID-19 incidence and prevalence. Water Res. 188, 116560 https://doi.org/10.1016/J.WATRES.2020.116560. Jan.

D\'Aoust, P.M., et al., 2021. COVID-19 wastewater surveillance in rural communities comparison of lagoon and pumping station samples. Sci. Total Environ. 801, 149618 https://doi.org/10.1016/J.SCITOTENV.2021.149618. Dec.

"Developing a Wastewater Surveillance Sampling Strategy | Water-related Topics | Healthy Water | CDC." https://www.cdc.gov/healthywater/surveillance/wastewater-surveillance/developing-a-wastewater-surveillance-sampling-strategy.html (Accessed 11 April 2022).

Ellison, S.L.R., English, C.A., Burns, M.J., Keer, J.T., 2006. Routes to improving the reliability of low level DNA analysis using real-time PCR. BMC Biotechnol. 6 (1), 1–11. https://doi.org/10.1186/1472-6750-6-33/FIGURES/5. Jul.

Feng, S., et al., 2021. Evaluation of sampling, analysis, and normalization methods for SARS-CoV-2 concentrations in wastewater to assess COVID-19 burdens in Wisconsin communities. ACS ES&T Water 1 (8), 1955–1965. https://doi.org/10.1021/ACSESTWATER.1C00160. Aug.

Fitzgerald, S.F., et al., 2021. Site specific relationships between COVID-19 cases and SARS-CoV-2 viral load in wastewater treatment plant influent. Environ. Sci. Technol. 55 (22), 15276–15286. https://doi.org/10.1021/ACS.EST.1C05029/SUPPL_FILE/ES1C05029_SI_001.PDF. Nov.

Forootan, A., Sjöback, R., Björkman, J., Sjögreen, B., Linz, L., Kubista, M., 2017. Methods to determine limit of detection and limit of quantification in quantitative real-time PCR (qPCR. Biomol. Detect. Quantif. 12, 1–6. https://doi.org/10.1016/J.BDQ.2017.04.001. June.

Ibrahim, N.K., 2020. Epidemiologic surveillance for controlling Covid-19 pandemic types, challenges and implications. J. Infect Public Health 13 (11), 1630–1638. https://doi.org/10.1016/J.JIPH.2020.07.019. Nov.

Kitajima, M., Sassi, H.P., Torrey, J.R., 2018. Pepper mild mottle virus as a water quality indicator. NPJ Clean Water 1 (1), 1–9. https://doi.org/10.1038/s41545-018-0019-5. Oct.

Larsen, D.A., Wigginton, K.R., 2020. Tracking COVID-19 with wastewater. Nat. Biotechnol. 38 (10), 1151–1153. https://doi.org/10.1038/S41587-020-0690-1. Oct.

Majowicz, S.E., et al., 2005. Estimating the under-reporting rate for infectious gastrointestinal illness in Ontario. Can. J. Public Health 96 (3), 178–181. https://doi.org/10.1007/BF03403685, 963May 2005.

Mallapaty, S., 2020. How sewage could reveal true scale of coronavirus outbreak. Nature 580 (7802), 176–177. https://doi.org/10.1038/D41586-020-00973-X. Apr.

Medema, G., Heijnen, L., Elsinga, G., Italiaander, R., Brouwer, A., 2020. Presence of SARS-Coronavirus-2 RNA in sewage and correlation with reported COVID-19 prevalence in the early stage of the epidemic in the Netherlands. Environ. Sci. Technol. Lett. 7 (7), 511–516. https://doi.org/10.1021/ACS.ESTLETT.0C00357/SUPPL_FILE/EZ0C00357_SI_001.PDF. Jul.

Michael-Kordatou, I., Karaolia, P., Fatta-Kassinos, D., 2020. Sewage analysis as a tool for the COVID-19 pandemic response and management the urgent need for ptimized protocols for SARS-CoV-2 detection and quantification. J. Environ. Chem. Eng. 8 (5), 104306 https://doi.org/10.1016/J.JECE.2020.104306. Oct.

O\'Reilly, K.M., Allen, D.J., Fine, P., Asghar, H., 2020. The challenges of informative wastewater sampling for SARS-CoV-2 must be met lessons from polio eradication. Lancet Microbe 1 (5), e189–e190. https://doi.org/10.1016/S2666-5247(20)30100-2. Sep.

Pellegrinelli, L., et al., 2016. Molecular Characterization and phylogenetic analysis of enteroviruses and hepatitis A viruses in sewage samples. Food Environ. Virol. 11 (4), 393–399. https://doi.org/10.1007/S12560-019-09401-4. Aug. 2019.

"Phase 1 Inter-Laboratory Study – Canadian Water Network." https//cwn-rce.ca/covid-19-wastewater-coalition/phase-1-inter-laboratory-study/(accessed Sep. 21, 2022).

Philo, S.E., et al., 2022. Development and validation of the skimmed milk pellet extraction protocol for SARS-CoV-2 wastewater surveillance. Food Environ. Virol. 1, 1–9. https://doi.org/10.1007/S12560-022-09512-5/FIGURES/3. Feb.

Pulicharla, R., Kaur, G., Brar, S.K., 2021. A year into the COVID-19 pandemic rethinking of wastewater monitoring as a preemptive approach. J. Environ. Chem. Eng. 9 (5), 106063 https://doi.org/10.1016/J.JECE.2021.106063. Oct.

Ramírez-Chavarría, R.G., et al., 2022. Loop-mediated isothermal amplification-based electrochemical sensor for detecting SARS-CoV-2 in wastewater samples. J. Environ. Chem. Eng. 10 (3), 107488 https://doi.org/10.1016/J.JECE.2022.107488. Jun.

Randazzo, W., Truchado, P., Cuevas-Ferrando, E., Simón, P., Allende, A., Sánchez, G., 2020. SARS-CoV-2 RNA in wastewater anticipated COVID-19 occurrence in a low prevalence area. Water Res. 181 https://doi.org/10.1016/J.WATRES.2020.115942. Aug.

"Real-time RT-PCR Primers and Probes for COVID-19 | CDC." https://www.cdc.gov/coronavirus/2019-ncov/lab/rt-pcr-panel-primer-probes.html (Accessed 21 September 2022).

Shah, S., Gwee, S.X.W., Ng, J.Q.X., Lau, N., Koh, J., Pang, J., 2022. Wastewater surveillance to infer COVID-19 transmission a systematic review. Sci. Total Environ. 804, 150060 https://doi.org/10.1016/J.SCITOTENV.2021.150060. Jan.

Shrivastava, A., Gupta, V., 2011. Methods for the determination of limit of detection and limit of quantitation of the analytical methods. Chron. Young Sci. 2 (1), 21. https://doi.org/10.4103/2229-5186.79345.

Symonds, E.M., Nguyen, K.H., Harwood, V.J., Breitbart, M., 2018. Pepper mild mottle virus a plant pathogen with a greater purpose in (waste)water treatment development and public health management. Water Res. 144, 1. https://doi.org/10.1016/J.WATRES.2018.06.066. Nov.

"Transmission of SARS-CoV-2 implications for infection prevention precautions." https://www.who.int/news-room/commentaries/detail/transmission-of-sars-cov-2-implications-for-infection-prevention-precautions (Accessed 28 March 2022).

Wu, F., et al., 2020. SARS-CoV-2 titers in wastewater are higher than expected from clinically confirmed cases,". mSystems 5 (4). https://doi.org/10.1128/MSYSTEMS.00614-20/ASSET/3176BDF3-0F21-4633-A5D6-65F5F9E59D15/ASSETS/GRAPHIC/MSYSTEMS.00614-20-F0004.JPEG. Aug.

Wu, S.L., et al., 2020. Substantial underestimation of SARS-CoV-2 infection in the United States. Nat. Commun. 11 (1), 1–10. https://doi.org/10.1038/s41467-020-18272-4, 111Sep. 2020.

Wu, F., et al., 2021. Wastewater surveillance of SARS-CoV-2 across 40 U.S. states from February to June 2020. Water Res. 202, 117400 https://doi.org/10.1016/J.WATRES.2021.117400. Sep.

Xagoraraki, I., O'Brien, E., 2020. Wastewater-based epidemiology for early detection of viral outbreaks. Springer, pp. 75–97.